



Contents lists available at ScienceDirect

Journal of Volcanology and Geothermal Research

journal homepage: www.elsevier.com/locate/jvolgeores

Fine ash content of explosive eruptions

W.I. Rose ^{a,*}, A.J. Durant ^{a,b,c}^a Geological Engineering and Sciences, Michigan Technological University, Houghton, MI 49931, USA^b School of Geographical Sciences/Department of Earth Sciences, University of Bristol, Bristol, UK^c Leverhulme Centre for Human Evolutionary Studies, University of Cambridge, UK

ARTICLE INFO

Available online xxxx

Keywords:

volcanic ash

hazards

grain size

ABSTRACT

In explosive eruptions, the mass proportion of ash that is aerodynamically fine enough to cause problems with jet aircraft or human lungs (<30 to 60 µm in diameter) is in the range of a few percent to more than 50%. The proportions are higher for silicic explosive eruptions, probably because vesicle size in the pre-eruptive magma is smaller than those in mafic magmas. There is good evidence that pyroclastic flows produce high proportions of fine ash by comminution and it is likely that this process also occurs inside volcanic conduits and would be most efficient when the magma fragmentation surface is well below the summit crater. Reconstructed total grain size distributions for several recent explosive eruptions indicate that basaltic eruptions have small proportions of very fine ash (~1 to 4%) while tephra generated during silicic eruptions contains large proportions (30 to >50%).

© 2009 Published by Elsevier B.V.

1. Introduction

1.1. Fine ash

In classical sedimentology, “volcanic ash” refers to pyroclasts with diameter, D , smaller than 2 mm (if $D > 2$ mm, *lapilli*). In this paper, we define the finest particle-size classes based on fluid-dynamic behavior and focus on particles that settle in non-turbulent flow regimes distinguished by low particle Reynolds numbers, R_e , where $R_e < 500$ (Bonadonna et al., 1998). This distinction is well-suited to this paper, as the focus of our study is the longer atmospheric residence time of fine and especially very fine ash. We use the term “fine ash” to include ash particles with diameters <1000 µm ($>0 \phi$) which fall in the intermediate flow regime ($0.4 < R_e < 500$), and “very fine ash” to include particles with diameter <30 µm ($>5 \phi$; $R_e < 0.4$) which settle according to Stokes Law in the *laminar flow* regime.

The terminal fall velocity of sedimenting particles, which determines residence time in the atmosphere, is sensitive to particle size and atmospheric conditions (these vary as a function of height – Fig. 1). Ash particles are not spherical, which complicates and further slows fallout (Riley et al., 2003). Ignoring the effect of shape for simplicity, we can define fine-ash particles in general terms as those with a predicted atmospheric residence time of >30 min and very fine ash particles with

residence times >3 h. In fact, we know that mass fractions of some volcanic ash events have particle diameters <10 µm which have predicted residence times of >10 days. Here we use the word “predicted” because we know that calculated fallout times based on settling according to Stokes Law are not accurate or are inaccurate for very fine ash which sediments much faster. Remote sensing results (Rose et al., 2000) and distal ash sampling studies (Durant et al., 2009–this volume) strongly suggest that both fine and very fine ash mostly fall within a day of their eruption, much faster than fluid dynamics modeling suggests.

1.2. Impacts of fine ash

Fine ash, and more importantly, very fine ash, have not been studied as much as coarse ash and lapilli. Distal ash deposits are generally dispersed over a more extensive area and at greater distance from the volcano, and form an ephemeral, irregular covering over a large area which may be quickly reworked and further dispersed by winds and rain. Sampling is difficult unless it is done during or immediately after fallout, and the fallout areas may be very large. Only a few eruptions have well-sampled very fine ash fallout (Table 1). Consequently, assessment of ash hazards is subject to large uncertainty because we know that two important hazards of volcanic ash are strongly-skewed toward very fine ash: (1) Human and animal health effects of ash, linked to respiratory illness, is closely associated with particle size, which are especially anticipated for diameters <10 µm (Horwell and Baxter, 2006) because aerodynamically fine particles successfully negotiate the curves of the throat and are carried

* Corresponding author.

E-mail address: raman@mtu.edu (W.I. Rose).

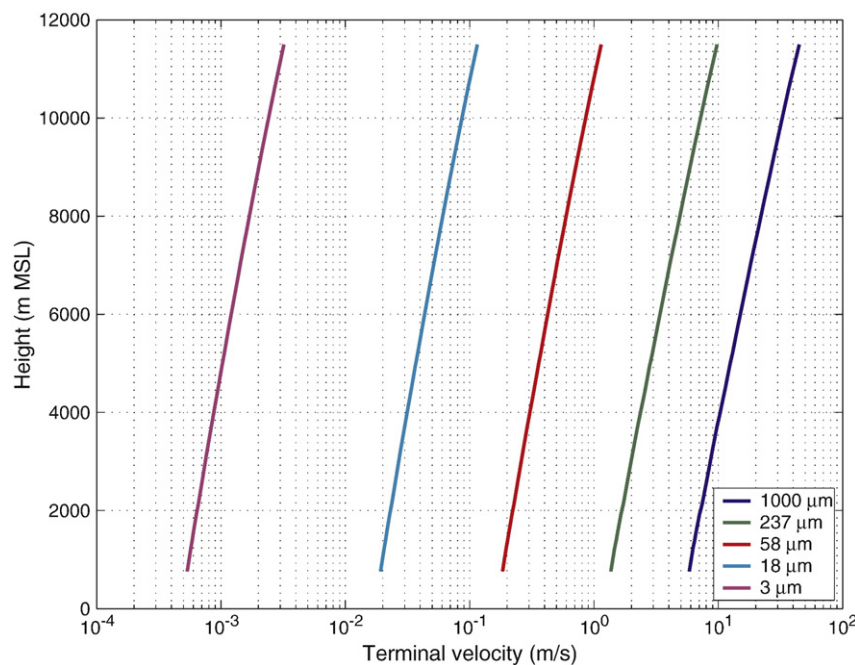


Fig. 1. Particle terminal fall velocities for spherical particles with density of 2300 kg m^{-3} calculated as a function of height in the atmosphere. Particle sizes correspond to subpopulation modes. Constraints on atmospheric conditions were taken from the sounding at Spokane International Airport (GEG) on 18 May 1980 at 18:00 UTC (from [Durant, 2007](#)).

to the lungs; and (2) aircraft operations (especially commercial jets) are threatened by volcanic cloud encounters, during which a variety of hazards exist such as airborne very fine ash that enters and melts in jet turbines and can cause failure ([Casadevall, 1994](#)).

1.3. Objectives

This paper aims to integrate new data about the origin and distribution of fine and very fine ash from the application of laser diffraction particle-size analysis (LDPSA) to fine and very fine volcanic ash-fall samples ([Table 1](#)). This data has been used to reconstruct the “total grain-size distribution” (TGSD) ([Bonadonna and Houghton, 2005](#)) of whole tephra deposits from some recent eruptions. This integration requires a spatial analysis of deposit grain-size distributions which are weighted according to deposit characteristics (either mass or thickness) to estimate the initial grain-size distribution before atmospheric fractionation ([Bonadonna and Houghton, 2005](#)). The details of this analysis are contained in the papers cited in [Table 1](#). TGSD can be used to assess potential hazards from explosive eruptions and will help address the following questions: (1) How is fine ash created? (2) What types of eruptions should create more fine ash? (3) What causes fine ash to fall faster than it would as simple particles? (4) What is the role of meteorology in this fallout? (5) Can this fallout be forecast?

2. Methods used

LDPSA determines the size distribution of a particle dispersion through the application of Mie theory or the Fraunhofer approximation to measured light scattering. Two instruments were used for this work which measure particle diameters from millimeter to submicron size: (1) Microtrac® SRA (Standard Range Analyzer) 9210-1-10-1 laser particle size analyzer and (2) Malvern Mastersizer 2000 laser particle size analyzer. The majority of very fine ash particles are smaller than standard sieve size classes and some of the most important data collected here using laser diffraction is in the “pan size” ($<63 \mu\text{m}$).

3. Results

Distal ash-fall particle size distributions are typically polymodal; the shapes of the distributions are neither well-sorted nor lognormal (e.g., [Fig. 2](#)). No single sample is representative of the size distribution generated in an eruption, because, in spite of the limited sorting evidenced by a single sample analysis, there is substantial sorting of lapilli and coarse ash that occurs during transport in the atmosphere. All processes, including fragmentation, and then during transport and deposition, must be assessed when evaluating a TGSD ([Wohletz et al., 1989](#)). As distance increases from the source volcano, particle sedimentation

Table 1

List of ash eruptions where LDPSA has been carried out to determine fine and very fine ash proportions. In this paper we use a subset of this list where total grain size distributions are better constrained

Eruption, date	Composition	Eruption type	Reference
Fuego, Guatemala 14 October 1974	Hi-Al basalt 51% SiO ₂	VEI 3–4 sub-plinian co-pf ash minor	Rose et al. (2007)
Crater Peak, Alaska, USA 18 August 1992	Andesite 56–58% SiO ₂	VEI 3 sub-plinian co-pf ash minimal	Durant and Rose (2009-this volume)
Crater Peak, Alaska, USA 16–17 September 1992	Andesite 56–58% SiO ₂	VEI 3 sub-plinian co-pf ash minimal	Durant and Rose (2009-this volume)
Colima, Mexico 2005–2006	Andesite 57–59% SiO ₂	VEI 1–2 separate vertical and co-pf ashes studied	Evans et al. (submitted for publication, 2008)
El Chichón, Mexico 4 April 1982	Trachyanandesite 55–57% SiO ₂	VEI 4–5 plinian abundant co-pf	Rose and Durant (2008)
Mount St. Helens, Washington, USA 18 May 1980	Dacite 64% SiO ₂	VEI 4–5 plinian abundant co-pf	Durant et al. (2008)
Pinatubo, Philippines 15 June 1991	Dacite 65% SiO ₂	VEI 6 plinian abundant co-pf	Darteville et al. (2002)
Bruneau–Jarbridge, USA 11 ka	Rhyolite 74% SiO ₂	VEI 8 major co-pf	Rose et al. (2003)

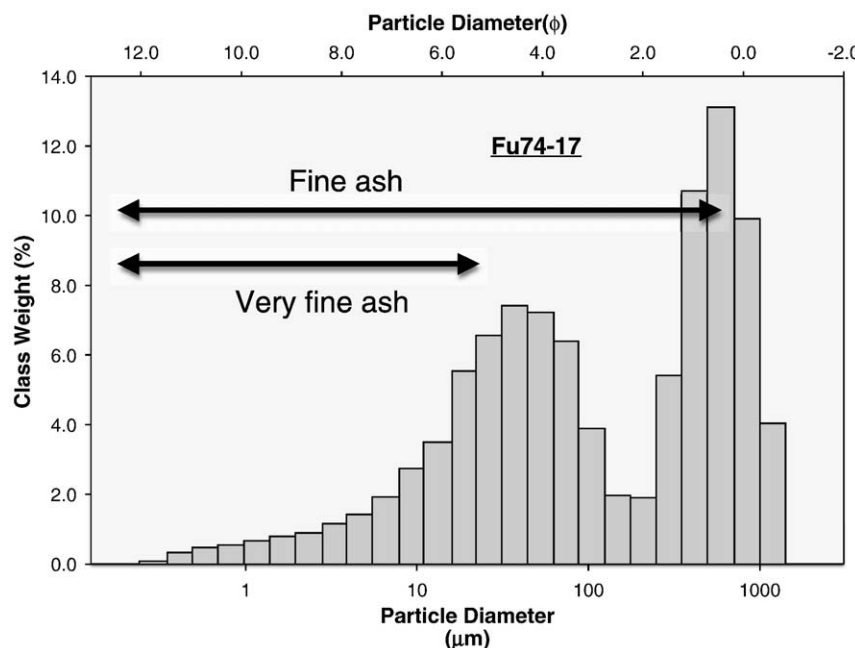


Fig. 2. Typical distal ash-fall particle size analysis from LDPSA techniques. Particle size distributions are typically polymodal and poorly-sorted. Grain size distribution data for a single fallout ash sample (VF 74-17) from the 14 October 1974 eruption of Fuego Volcano, Guatemala (Rose et al., 2007). This is presented to show a typical example of the large number of individual ash-fall samples studied to obtain total grain size distributions. Note that this sample, typical of the majority studied, does not contain a single mode of sizes, but has a larger mode which is symmetrical on a log-normal histogram and a fine mode which is fine-skewed. The sample overall has a high proportion (~50%) of very fine ash. Also note that LDPSA provides a way to describe the size distribution below about 63 μm , where sieves become difficult to use. The graphical software used here is Gradistat (Blott and Pye, 2001).

transitions from inertial-dominated single particle settling to aggregation-dominated very fine particle settling. The deposit reflects this shift through a change in the abundance of particle size subpopulations related to specific processes (Fig. 3). Particle size distributions exhibit a coarse particle subpopulation that fines and reduces in proportion as distance from the volcano increases (Pyle, 1989), but also a finer subpopulation (mode at about 4–5 ϕ , 31–62 μm diameter) that retains consistent size characteristics, but becomes proportionally-dominant in distal regions of the deposit (Durant et al., 2009-this volume).

Fig. 4 shows data from the 14 October 1974 eruption of Fuego, Guatemala, which is used as a demonstration of TGSD reconstruction. Each ash sample collected in the field has deposit thickness and a measured size distribution (Table 2). All data are weighted to reconstruct a TGSD for the whole eruption, in this case by isopach volume (Murrow et al., 1980) or Voronoi tessellation (Bonadonna and Houghton, 2005). Following the Murrow et al. approach, total mass erupted consists of ~64% fine ash and ~4% very fine ash.

In the case of more explosive eruptions where dispersion is higher, e.g., 18 May 1980 eruption of Mount St. Helens, the determination of a total grain size distribution is much more challenging. Durant et al. (2009-this volume) have presented new LDPSA data for the extensive fall blanket studied by Sarna-Wojcicki et al. (1981) which allow for reevaluation of the TGSD. All details of that data are not included here but we do include some detail to show where uncertainty is most obvious. The fall deposit produced an elongate deposit which thinned to the east but contained a secondary maximum of thickness and mass at a distance of 330 km along the dispersal axis. Greater than 90% of the fallout was finer than 100 μm in diameter and did not change much after about 300 km (Durant et al., 2009-this volume). Total grain size distribution of the MSH80 deposit was reconstructed (Fig. 5) following several approaches to provide weight to individual measurements: (1) “volume” – isopach interval volume-weighted (Murrow et al., 1980); (2) “mass” and “carey” – mass-weighted as a function of distance (Carey and Sigurdsson, 1982); and (3) “voronoi” – using Voronoi tessellation to weight individual analyses (Bonadonna and Houghton, 2005). In both

techniques, the deposit is segregated into regions and particle size distributions of samples in a given region are combined and averaged, and given weight before being combined to generate the total particle size distribution. Deposit volume was estimated using both incremental and integration techniques (Rose et al., 1973; Pyle, 1989). Similar procedures were followed to determine TGSD for several of the eruptions of Table 1 and these are shown in Figs. 6 and 7. Note that all of the eruptions shown here have important modes in the very fine ash range, finer than 4–5 ϕ (31–62 μm diameter), as observed for Fuego 1974. The more silicic and higher VEI eruptions have a dominance of very fine ash modes, with peaks at 5–7 ϕ (8–31 μm diameter). These relationships provide some guidance for volcanic cloud hazards, as explained by Mastin et al. (2009-this volume).

Calculated bulk deposit volume ranges from 0.70 km^3 for the incremental approach (Murrow et al., 1980), 1.00 km^3 for the exponential approach (Pyle, 1989), and 1.75 km^3 for the power law technique (Bonadonna and Houghton, 2005). Using an average bulk density for the deposit of 450 kg m^{-3} (Sarna-Wojcicki et al., 1981), total mass erupted is between 3.1×10^{11} kg to 7.9×10^{11} kg (this compares to 4.9×10^{11} kg to 5.5×10^{11} kg as calculated by Sarna-Wojcicki et al. (1981)). Assuming a glass density of 2300 kg m^{-3} , dense rock equivalent volume (DRE) ranged from 0.13–0.34 km^3 (which compares to 0.20–0.25 km^3 as calculated by Sarna-Wojcicki et al. (1981)). These calculations only include thickness data out to the 0.5 mm isopach contour, so they underestimate the actual volume.

The incremental technique underestimates volume as thickness is not interpolated between isopach contours and the calculation only includes isopach regions down to 0.5 mm thickness. Extending the isopach map beyond this to locations of zero thickness may generate an additional 25% in deposit area. Although these approaches do allow a framework for estimating the mass of material beyond the area mapped, both the exponential and power law techniques tend to obscure deposit thickness variations over the distal mass deposition maximum. Finally, fallout was mapped only as far as ~700 km from the volcano; the deposit continued further to the east, so some proportion of fine material has not

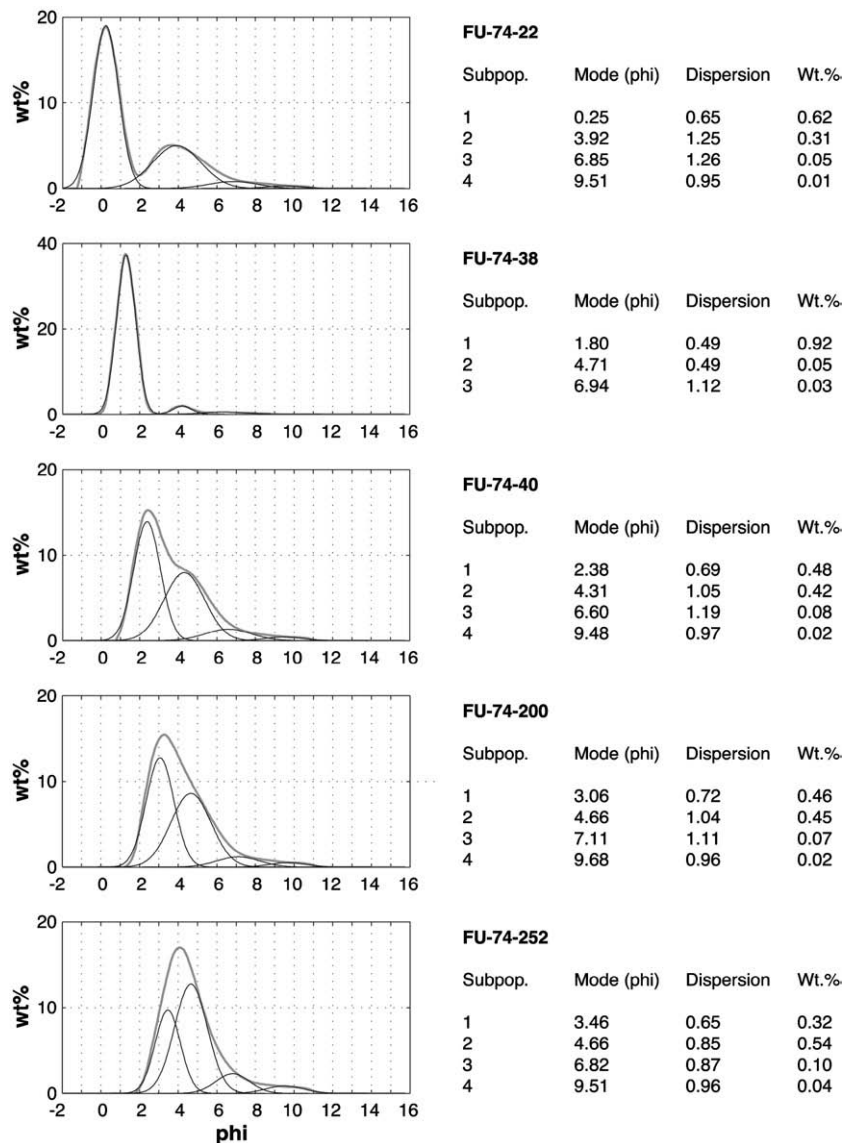


Fig. 3. Several samples of ash-fall from the 10 Oct 1974 ash-fall of Fuego (Rose et al., 2007) which have been analyzed by SFT methods (Wohletz et al., 1989) arranged by distance, to show the effects of atmospheric fractionation. The coarse mode diminishes with distance but the fine mode persists.

been accounted for in these calculations. Rose et al. (2007) speculate that this “missing” fraction may account for 6–33% of the total mass erupted in the case of the 14 October 1974 eruption of Fuego, Guatemala, and overall the differences in total mass obtained by the different methods show that this missing fraction may be even higher for the more explosive MSH80 case and other silicic and explosive eruptions.

4. Discussion

4.1. Production of fine and very fine ash

Pyroclasts are fragments of magma which form by a variety of processes such as rapid decompression and explosive vesiculation. During ascent in the crust, gas exsolves from magma and forms bubbles which coalesce and form an over-pressurized foam that ruptures explosively (Alidibirov and Dingwell, 1996). Hydromagmatic processes, where magma comes in contact with external water during eruption, may also produce ash in some circumstances. Large pyroclasts can be further reduced in size after primary fragmentation through comminution

or “milling” in the volcano conduit or pyroclastic flows. The pyroclastic flow milling process was advocated by Darteville et al. (2002) to explain the overall fine-grained character of the 15 June 1992 Pinatubo tephra-fall deposit. During recent eruptions at Colima volcano, Mexico, milling in the pyroclastic flows was inferred by a predominance of very fine co-ignimbrite ash elutriated from pyroclastic flows, compared to compositionally similar ash from equivalent vertical eruption plumes (Evans et al., submitted for publication, 2008). An important test of the efficacy of the milling is the crystal concentration relationships which can be demonstrated between large pumices and pyroclastic flow matrix samples (Walker, 1981).

Silicic eruptions tend to have higher proportions (30% to >50%) of fine particles <100 µm, which may reflect enhanced comminution, either in pyroclastic flows (e.g., 1980 Mount St. Helens and 1982 El Chichón eruptions) or in the conduit following explosive fragmentation (e.g., 1992 Spurr eruptions). In contrast, the 1974 Fuego eruption produced a sustained column for ~5 h, but erupted about an order of magnitude less material than MSH80 and had a low proportion of very fine particles (<4%). Other small scale mafic eruptions where total

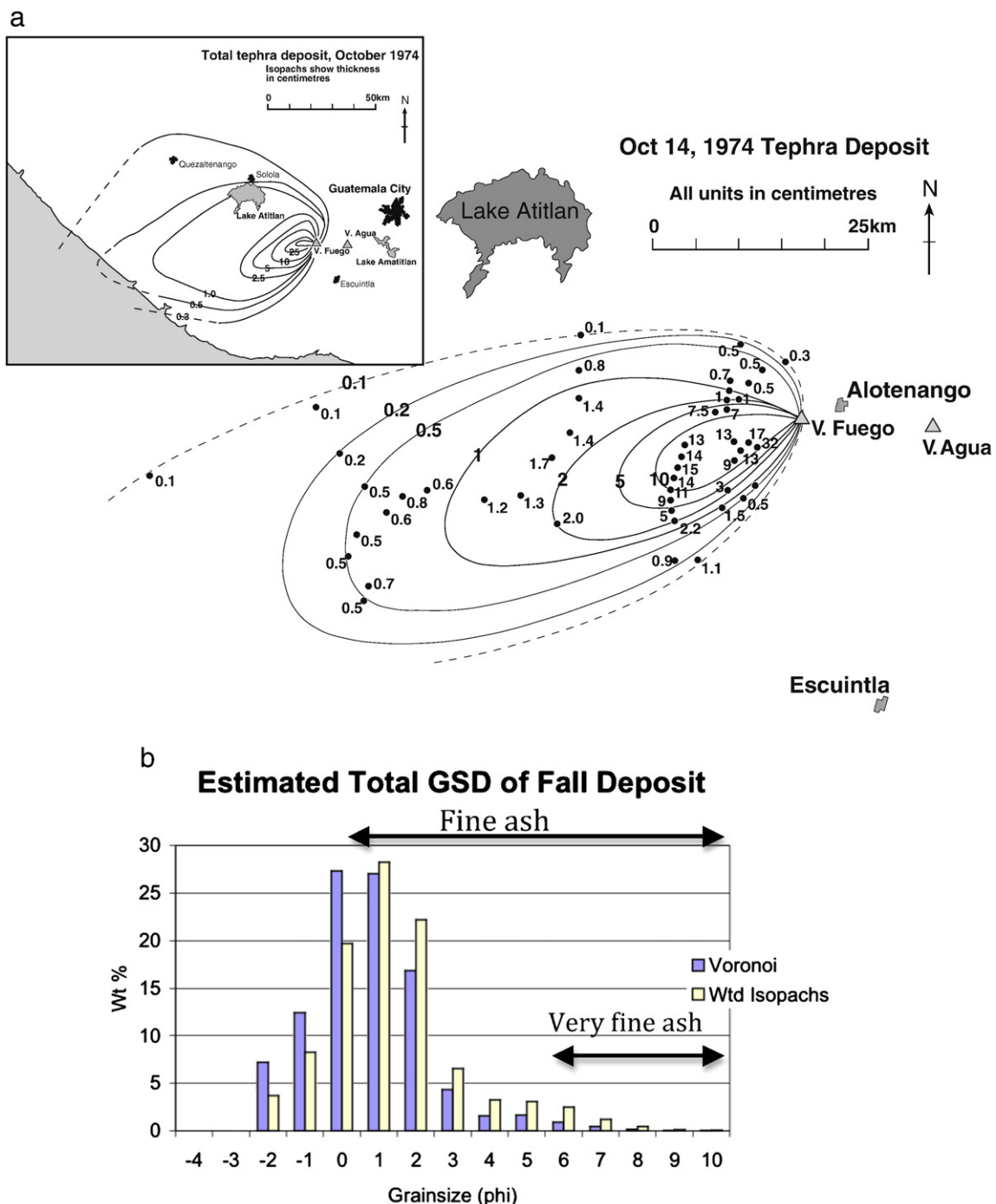


Fig. 4. Isopach map of 14 Oct 1974 fall deposit from Fuego Volcano, Guatemala. The individual points on the map are ash sample locations where thickness and particle size determinations were made. All particle size data is weighted based on isopach region or the Voronoi method (Bonadonna and Houghton, 2005). This figure material is explained fully in Rose et al. (2007). Note that this eruption overall produced about 56–64% fine ash by mass and only 2–4% very fine ash.

grain size analysis has been completed were compiled by Mastin et al. (2009-this volume) and indicate low proportions (a few percent) of very fine particles. The low abundance of very fine material probably results from the lower viscosity of the pre-eruptive magma (lower over-pressure and less energetic fragmentation generating less primary particles). It is likely that more explosive eruptions generate a higher proportion of fine ash due to the presence of more numerous and smaller, highly over-pressured bubbles. It is also true that explosive silicic eruptions are more likely to be accompanied by major pyroclastic flows which produce huge quantities of fine ash and

elutriate it, generating *phoenix* or *coignimbrite* clouds. This connection is important and indicates that coignimbrite-dominated activity is potentially more hazardous in terms of the amount of fine material generated during an eruption. The TGSD shown in Figs. 4–7 generally agree with these ideas for pyroclast formation, and demonstrate a correlation between eruption intensity (VEI in Table 1), silica percentage and the proportion of very fine ash.

Particle subpopulations were discriminated in the MSH80 TGSD following the approach of Wohletz et al. (1989): average modes were located at $-3.31\ \Phi$ ($9925.4\ \mu\text{m}$), $-1.83\ \Phi$ ($3633.7\ \mu\text{m}$), $-0.17\ \Phi$ ($1128.5\ \mu\text{m}$),

Table 2

Proportions of fine and very fine ash determined from TGSD reconstructions for selected eruptions. All reconstructions were carried out following the Murrow et al. (1980) approach, or the Bonadonna and Houghton (2005) if indicated by "Voronoi". The ranges in proportions for El Chichón 1982 and Mount St. Helens 1980 are related to different assumptions about isopach areas used for weighting the reconstruction

Eruption	Fine ash (>0 phi/<1000 µm) wt.%	Very fine ash (>5 phi/<31 µm)
Fuego, Guatemala 14 October 1974	56.1 (Voronoi) 64.2	1.6 (Voronoi) 4.2
Crater Peak, Alaska, USA 18 August 1992	79.1	18.1
Crater Peak, Alaska, USA 16–17 September 1992	83.8	23.3
El Chichón, Mexico 4 April 1982	93.6–95.8	29.0–48.4
Mount St. Helens, Washington, USA 18 May 1980	95.7–97.2	44.6–51.5

1.60 φ (350.5 µm), 5.34 φ (24.9 µm) and 9.03 φ (1.9 µm) (Durant et al., 2009–this volume). Some of the particle subpopulations in MSH80 fallout may be related to explosive vesiculation. Analysis of MSH80 pumice clasts indicated there were 2 vesicle populations with modes at 50 µm (white) and 15 µm (gray) (Klug and Cashman, 1994), which compares to particle size subpopulations with modes at 58 µm and 18 µm. In addition, direct observation from scanning electron microscopy indicates that vesicles in tephra are rarely smaller than 5 µm and thermodynamics suggest a minimum size of ~1 µm (Sparks, 1978), which compares to the finest subpopulation.

4.2. The fate of very fine ash

Very fine ash is transported in volcanic clouds, often in the upper troposphere or lower stratosphere where it presents a hazard to jet aircraft. Remote sensing detection methods, such as the split window technique, are able to measure the distribution of ash in transparent volcanic clouds containing particles with diameter <25 µm (Wen and Rose, 1994). Combined studies have shown that volcanic cloud ash mass decreases by an order of magnitude in 24 h (Rose et al., 2000). This rapid fallout of very fine ash creates distal mass deposition maxima in tephra deposits at distances several 100s of km downwind (Brazier et al., 1983; Durant and Rose, this volume). The distal ash sedimentation process is poorly understood but is clearly tied to meteorological processes that promote aggregation, e.g., hydrometeor formation, and influence cloud dynamics, e.g., mammatus formation (Durant et al., 2009–this volume).

A common goal is to improve forecasts of distal ash fallout, both to mitigate hazards to aviation and on the ground (fall hazards, and human and animal health). A step towards successful ash dispersion and transport forecasts involves constraining possible fine ash proportions contained in volcanic clouds soon after emplacement into the atmosphere. Very fine ash masses and realistic deposition rates may be included as input to 3-D atmospheric trajectory models used to predict ash transport and fallout. Taking this as motivation, Mastin et al. (2009–this volume) derive the parameter m_{63} from total GSD data, such as that in Figs. 4–7, to describe the mass of very fine ash generated by different eruptive styles. Additionally, the work here suggests that the severity of hazards are correlated to the explosivity of eruptive events, especially to the occurrence of pyroclastic flows. Better understanding of the fallout process is critical to accurately forecast hazardous fallout of very fine ash.

5. Conclusions

TGSD from several recent eruptions have been reconstructed from LDPSA of extensively sampled tephra fallout blankets. The data indicate that eruptions generate fallout with polymodal particle size distributions, which includes substantial proportions of particles <30 µm (very fine ash) with particular significance to hazards. This material is more abundant in highly silicic explosive eruptions and those with prominent pyroclastic flows.

Since the coarse fractions of pyroclasts have short atmospheric residence times due to rapid sedimentation, it is the very fine particles with extended atmospheric residence times that present the greatest

hazard. Distal ash sedimentation is linked to meteorological processes that enhance particle aggregation and generate large scale cloud subsidence. It is possible that meteorological data collected in near-real-time may provide constraints that will lead to successful fallout forecasts for fine and very fine ash.

Acknowledgements

Andrei Sarna-Wojcicki and Elmira Wan are thanked for providing access and assistance with the 18 May 1980 Mount St. Helens samples. The University of Cambridge Malvern Laboratory and staff are thanked for assistance with some of the LDPSA analyses. Komar Kawatra kindly provided access to Michigan Tech's Microtrac lab. AJD gratefully acknowledges support during the final preparation of this manuscript as a member of the GREENCYCLES Marie Curie Research Training Network. Alain Volentik helped with voronoi tessellation analysis.

References

- Alidibirov, M., Dingwell, D.B., 1996. Magma fragmentation by rapid decompression. *Nature* 380 (6570), 146–148.
- Blott, S.J., Pye, K., 2001. Gradistat: a grain size distribution and statistics package for the analysis of unconsolidated sediments. *Earth Surface Processes and Landforms* 26 (11), 1237–1248.
- Bonadonna, C., Houghton, B.F., 2005. Total grain-size distribution and volume of tephra fall deposits. *Bulletin of Volcanology* 67 (5), 441–456.
- Bonadonna, C., Ernst, G.G.J., Sparks, R.S.J., 1998. Thickness variations and volume estimates of tephra fall deposits: the importance of particle Reynolds number. *Journal of Volcanology and Geothermal Research* 81 (3–4), 173–187.
- Brazier, S., Sparks, R.S.J., Carey, S.N., Sigurdsson, H., Westgate, J.A., 1983. Bimodal grain size distribution and secondary thickening in air-fall ash layers. *Nature* (London) 301 (5896), 115–119.
- Carey, S.N., Sigurdsson, H., 1982. Influence of particle aggregation on deposition of distal tephra from the May 18, 1980, eruption of Mount St. Helens volcano. *Journal of Geophysical Research* 87 (B8), 7061–7072.
- Casadevall, T.J., 1994. Volcanic ash and aviation safety: proceedings of the first international symposium, Seattle, Washington, July 1991. US Geological Survey Bulletin 2047, 450.
- Darteville, S., Ernst, G.G.J., Bernard, A., 2002. Origin of the Mount Pinatubo climactic eruption cloud: implications for volcanic hazards and atmospheric impacts. *Geology* 30 (7), 663–666.
- Durant, A.J., 2007. On Water in Volcanic Clouds. Ph.D. Thesis, Michigan Technological University, Houghton, Michigan, 242 pp.
- Durant, A.J., Rose, W.I., 2009–this volume. Sedimentological constraints on hydrometeor-enhanced particle deposition: 1992 eruptions of Crater Peak, Alaska. *Journal of Volcanology and Geothermal Research*.
- Durant, A.J., Rose, W.I., Sarna-Wojcicki, A.M., Carey, S., Volentik, A.C., 2009–this volume. Hydrometeor-enhanced tephra sedimentation from the 18 May 1980 Mount St. Helens (USA) volcanic cloud. *Journal of Geophysical Research*.
- Durant, A.J., Shaw, R.A., Rose, W.I., Mi, Y., Ernst, G.G.J., 2008. Ice nucleation and overseeding of ice in volcanic clouds. *Journal of Geophysical Research* 113. doi:10.1029/2007JD009064.
- Evans, J.R., Huntton, J.E., Rose, W.I., Varley, N.R., submitted for publication. Characteristics of ash deposits derived from vertical explosions and co-pyroclastic flow clouds, Volcán de Colima, Mexico. *Geology*.
- Horwell, C., Baxter, P., 2006. The respiratory health hazards of volcanic ash: a review for volcanic risk mitigation. *Bulletin of Volcanology* 69 (1), 1–24.
- Klug, C., Cashman, K.V., 1994. Vesiculation of May 18, 1980, Mount St. Helens magma. *Geology* 22, 468–472.
- Mastin, L.G., Guffanti, M., Servranckx, R., Webley, P., Barsotti, S., Dean, K., Durant, A., Ewert, J.W., Neri, A., Rose, W.I., Schneider, D., Siebert, L., Stunder, B., Swanson, G., Tupper, A., Volentik, A., Waythomas, C.F., 2009–this volume. A multidisciplinary effort to assign realistic source parameters to models of volcanic ash-cloud transport and dispersion during eruptions. *Journal of Volcanology and Geothermal Research*.

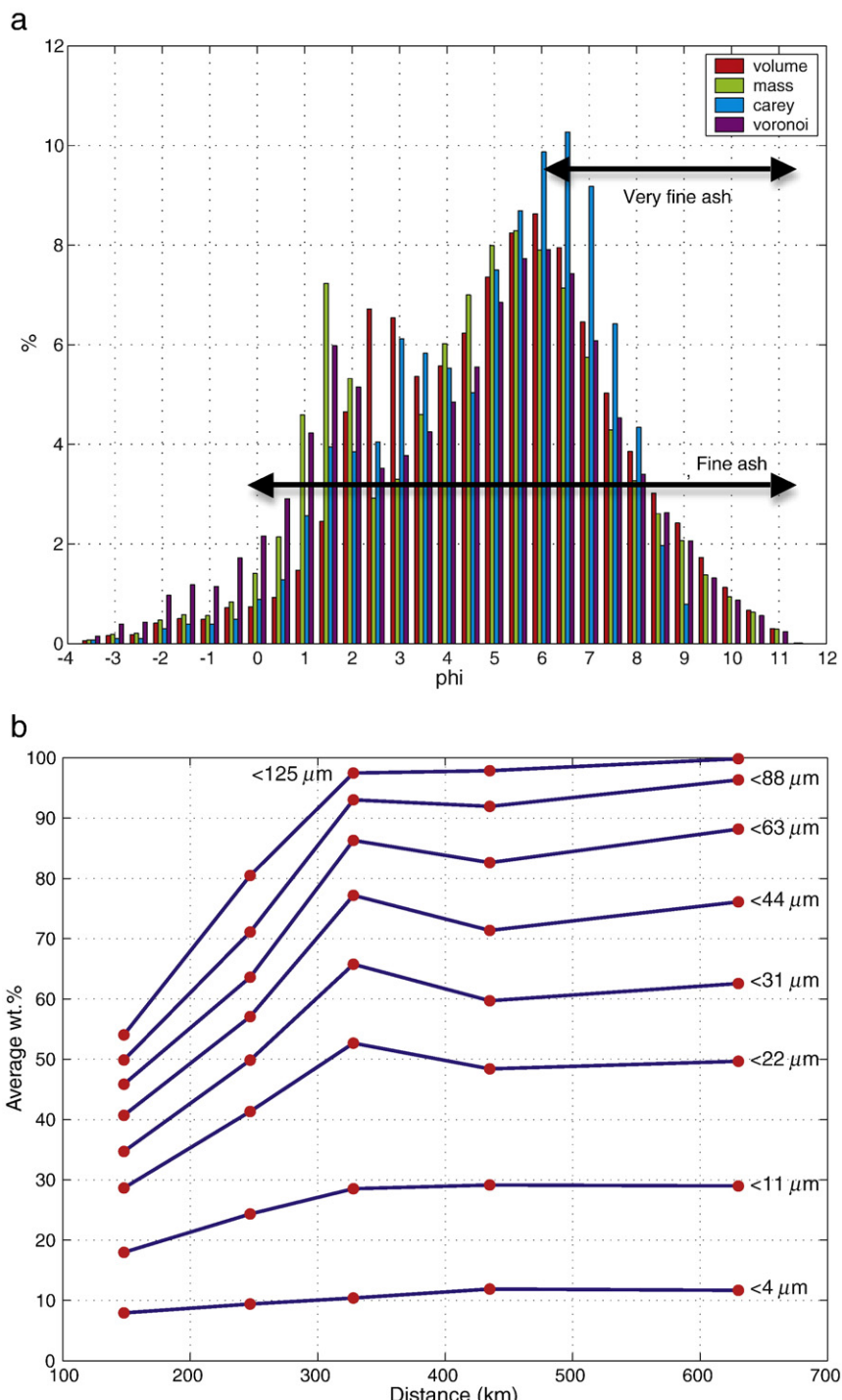


Fig. 5. TGSD of 18 May 1980 Mount St. Helens eruption weighted by mass, by isopach volume and using the Voronoi method (reconstructed up to 670 km from the volcano), and compared with values determined independently by Carey and Sigurdsson (1982) (reconstructed up to 500 km from the volcano). Note that the proportions of fine ash ($>0 \phi$; $>95\%$) and very fine ash ($>5 \phi$; $>80\%$) are very high regardless of the TGSD weighting scheme used.

- Murrow, P.J., Rose Jr., W.I., Self, S., 1980. Determination of the total grain size distribution in a vulcanian eruption column, and its implications to stratospheric aerosol perturbation. *Geophysical Research Letters* 7 (11), 893–896.
- Pyle, D.M., 1989. The thickness, volume and grain size of tephra fall deposits. *Bulletin of Volcanology* 51 (1), 1–15.
- Riley, C.M., Rose, W.I., Bluth, G.J.S., 2003. Quantitative shape measurements of distal volcanic ash. *Journal of Geophysical Research* 108 (B10), ECV 8–1.
- Rose, W.I., Durant, A.J., 2008. El Chichón volcano, 4 April 1982: volcanic cloud history and fine ash fallout. *Natural Hazards*. doi:10.1007/s11069-008-9283-x.
- Rose, W.I., Bonis, S., Stoiber, R.E., Keller, M., Bickford, T., 1973. Studies of volcanic ash from two recent Central American eruptions. *Bulletin Volcanologique* 37 (3), 338–364.
- Rose, W.I., Bluth, G.J.S., Ernst, G.G.J., 2000. Integrating retrievals of volcanic cloud characteristics from satellite remote sensors: a summary. *Philosophical Transactions of the Royal Society of London Series a—Mathematical Physical and Engineering Sciences* 358 (1770), 1585–1606.

- Rose, W.I., Riley, C.M., Darteville, S., 2003. Sizes and shapes of 10-Ma distal fall pyroclasts in the Ogallala Group, Nebraska. *Journal of Geology* 111 (1), 115–124.
- Rose, W., et al., 2007. Nature and significance of small volume fall deposits at composite volcanoes: insights from the October 14, 1974 Fuego eruption, Guatemala. *Bulletin of Volcanology*. doi:10.1007/s00445-007-0187-5.
- Sarna-Wojcicki, A.M., et al., 1981. Areal distribution, thickness, mass, volume, and grain size of air-fall ash from the six major eruptions of 1980. In: Lipman, P.W., Mullineaux, D.R. (Eds.), *The 1980 Eruptions of Mount St. Helens, Washington*. U. S. Geological Survey, Reston, VA, pp. 577–600.
- Sparks, R.S.J., 1978. The dynamics of bubble formation and growth in magmas: a review and analysis. *Journal of Volcanology and Geothermal Research* 3 (1–2), 1–37.

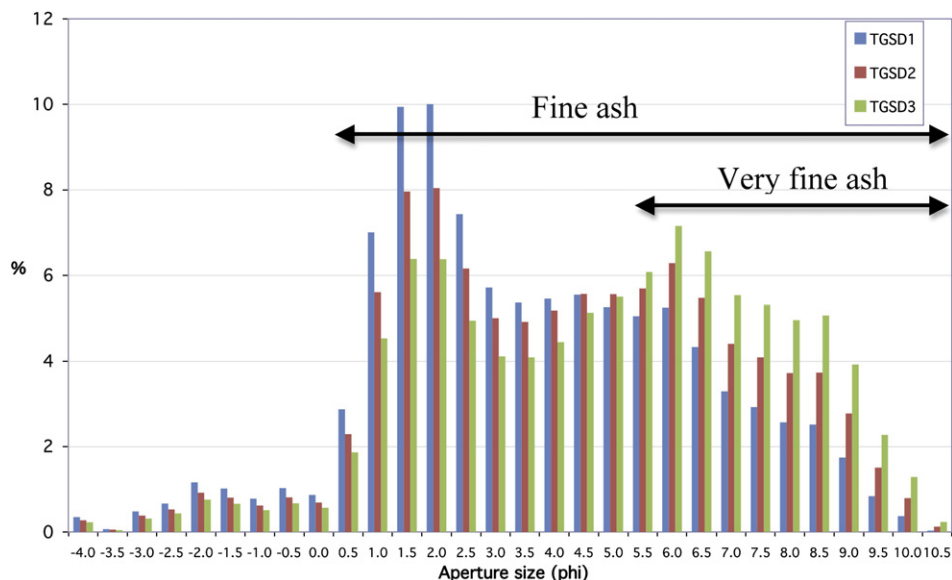


Fig. 6. TGSD of 4 April 1982 eruption of El Chichón, Mexico (Rose and Durant, 2008). The three versions reflect uncertainty in the amounts of distal ash because of inadequate sampling density. The cases "5 vol.%" "25 vol.%" and "50 vol.%" reflect a weighting accounting for 5, 25 and 50 vol.% outside the 0.2 cm isopach. Note that for this eruption fine ash makes up >95% and very fine ash >60%. These proportions are similar to the Mount St. Helens data in Fig. 5.

Walker, G.P.L., 1981. Generation and dispersal of fine ash and dust by volcanic eruptions. *Journal of Volcanology and Geothermal Research* 11, 81–92.

Wen, S., Rose, W.I., 1994. Retrieval of sizes and total masses of particles in volcanic clouds using AVHRR bands 4 and 5. *Journal of Geophysical Research* 99, 5421–5431.

Wohletz, K.H., Sheridan, M.F., Brown, W.K., 1989. Particle-size distributions and the sequential fragmentation transport-theory applied to volcanic ash. *Journal of Geophysical Research—Solid Earth and Planets* 94 (B11), 15703–15721.

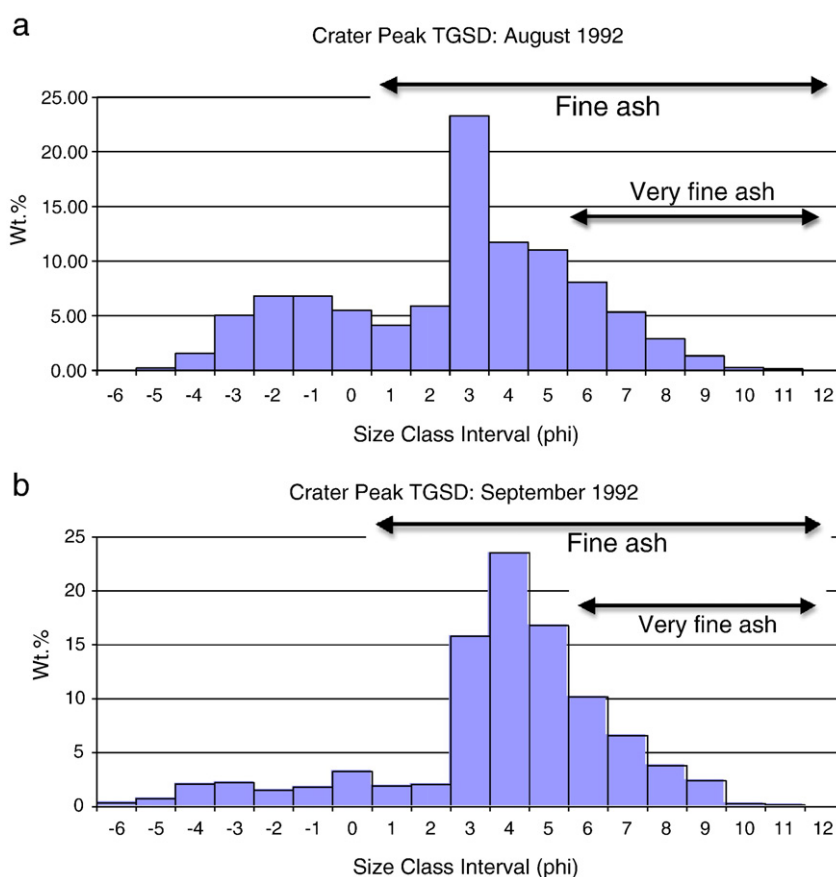


Fig. 7. Total grain size distributions for two 1992 eruptions of Crater Peak, Mount Spurr, Alaska (Durant and Rose, this volume).